

## Supplementary Information

### Facile Synthesis of Hemiacetal Ester-based Dynamic Covalent Polymer Networks Combining Fast Reprocessability and High Performance

Hongzhi Feng<sup>1, 2</sup>, Songqi Ma<sup>1\*</sup>, Xiwei Xu<sup>1, 2</sup>, Qiong Li<sup>1, 2</sup>, Binbo Wang<sup>1, 2</sup>, Na Lu<sup>1, 2</sup>, Pengyun Li<sup>1, 2</sup>, Sheng Wang<sup>1, 2</sup>,  
Zheng Yu<sup>1</sup>, Jin Zhu<sup>1</sup>

<sup>1</sup>Key Laboratory of Bio-based Polymeric Materials Technology and Application of Zhejiang Province, Laboratory of Polymers and Composites, Ningbo Institute of Materials Technology and Engineering, Chinese Academy of Sciences, Ningbo 315201, P. R. China;

<sup>2</sup>University of Chinese Academy of Sciences, Beijing 100049, P. R. China;

\*Corresponding authors: (Songqi Ma) E-mail masongqi@nimte.ac.cn, Tel 86-574-87619806.

## Contents

Fig. S1 FTIR spectra of PMMCs.....	3
Fig. S2 $^1\text{H}$ NMR spectrum of IBA-CVE.....	3
Fig. S3 $^{13}\text{C}$ NMR spectrum of IBA-CVE.....	4
Fig. S4 $^1\text{H}$ NMR spectrum of PPA-IVE.....	4
Fig. S5 $^{13}\text{C}$ NMR spectrum of PPA-IVE.....	5
Fig. S6 $^1\text{H}$ NMR spectrum of IBA-IVE .....	5
Fig. S7 $^{13}\text{C}$ NMR spectrum of IBA-IVE .....	6
Fig. S8 $^1\text{H}$ NMR spectrum of PPA-CVE .....	6
Fig. S9 $^{13}\text{C}$ NMR spectrum of PPA-CVE .....	7
Fig. S10 Stress relaxation curves of PMMC-5 at different temperatures.....	7
Fig. S11 Stress relaxation curves of PMMC-10 at different temperatures.....	7
Fig. S12 Stress relaxation curves of PMMC-15 at different temperatures.....	8
Fig. S13 Stress relaxation curves of PMMC-20 at different temperatures.....	8
Fig. S14 Reprocess recycling through hot press with different time.....	9
Fig. S15 Frequency sweep measurements at 150 °C of the original and reprocessed (compression remolded) PMMC-10.....	9
Fig. S16 Reprocess recycling through extrusion plastometer and hot press at 160 °C for 10 min.....	10
Fig. S17 Representative tensile stress-strain curves of the original and reprocessed PMMC-5.....	10
Fig. S18 Representative tensile stress-strain curves of the original and reprocessed PMMC-10.....	10
Fig. S19 Representative tensile stress-strain curves of the original and reprocessed PMMC-15.....	11
Fig. S20 Representative tensile stress-strain curves of the original and reprocessed PMMC-20.....	11
Fig. S21 Time sweep measurement at 120 °C of the PMMC-10.....	11
Fig. S22 Mass spectra of PPA-IVE, IBA-CVE, IBA-IVE, PPA-CVE .....	12
Fig. S23 Gas chromatograms of metathesis without PPA at 120 °C for different time.....	12
Fig. S24 Gas chromatograms of metathesis with PPA at 60 °C for different time.....	13
Fig. S25 Fraction of 1 as a function of time during the exchange experiment at different temperatures .....	13
Fig. S26 Plot of $-\ln ([1] [1]_0)$ versus t for the small molecule 1. $k_{exp}$ at each temperature was determined by its slope value.....	14
Fig. S27 Arrhenius analysis of the rate constant $k_{exp}$ versus T for 1 and 2 exchange .....	14
Table S1 Mechanical properties of different samples .....	15
Table S2 Thermo-physical properties of different samples .....	15
Table S3 Mechanical properties of the original and reprocessed PMMC-5 .....	15
Table S4 Transition state geometry.....	16

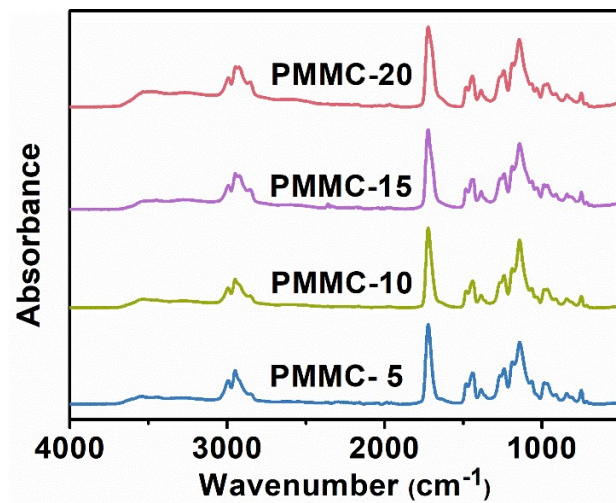


**Fig. S1** FTIR spectra of PMMCs.

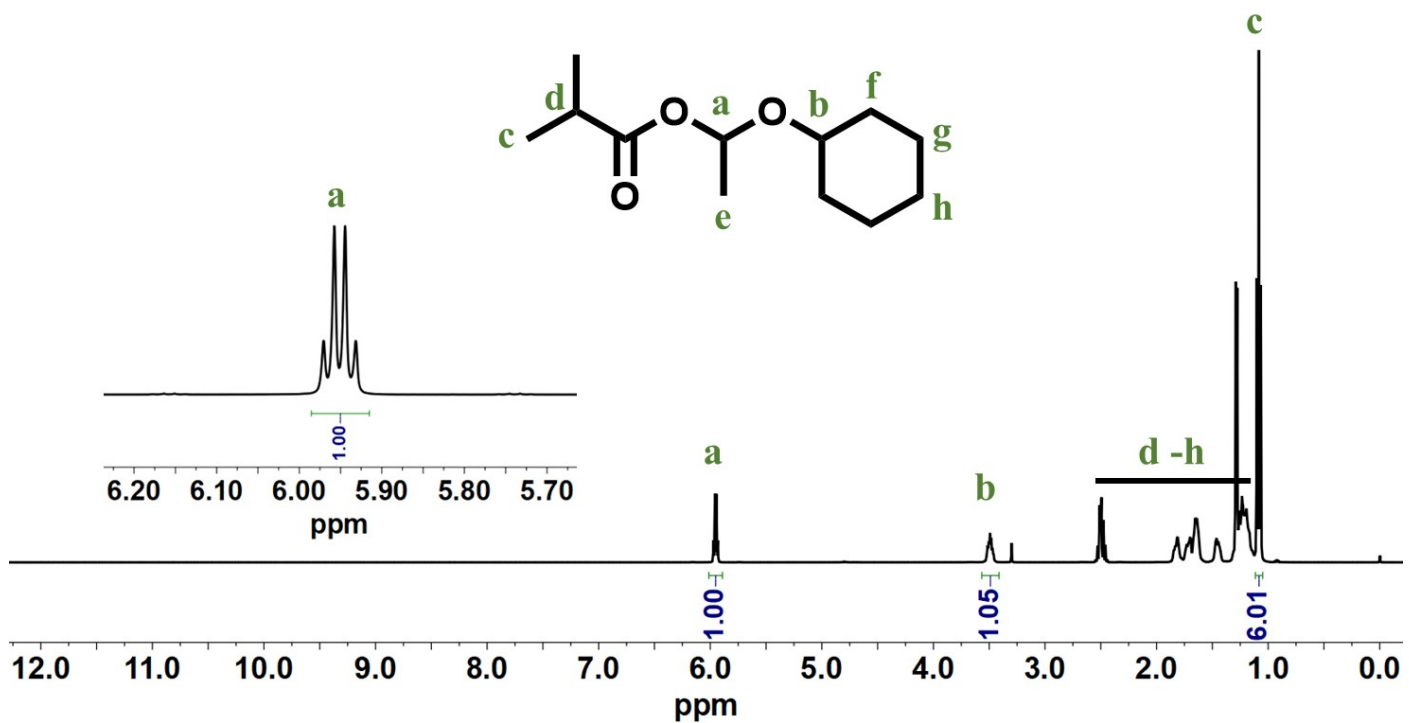


**Fig. S2**  $^1\text{H}$  NMR spectrum of IBA-CVE.

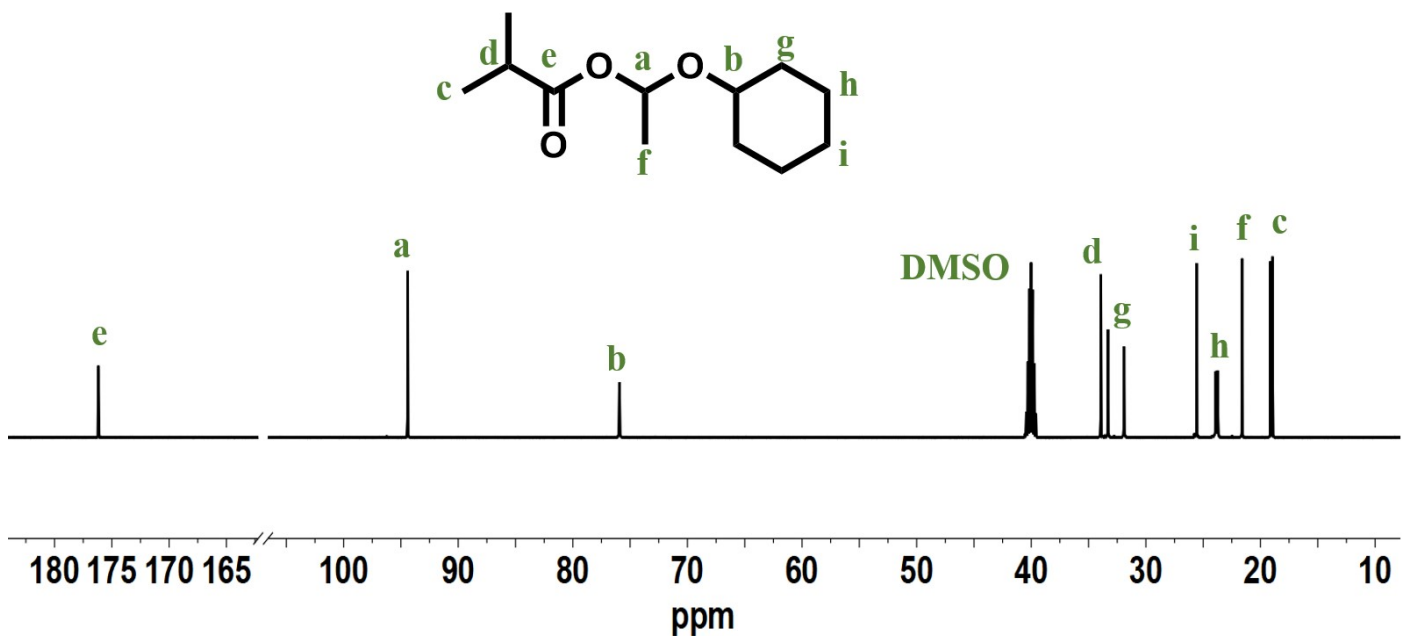


**Fig. S3**  $^{13}\text{C}$  NMR spectrum of IBA-CVE.

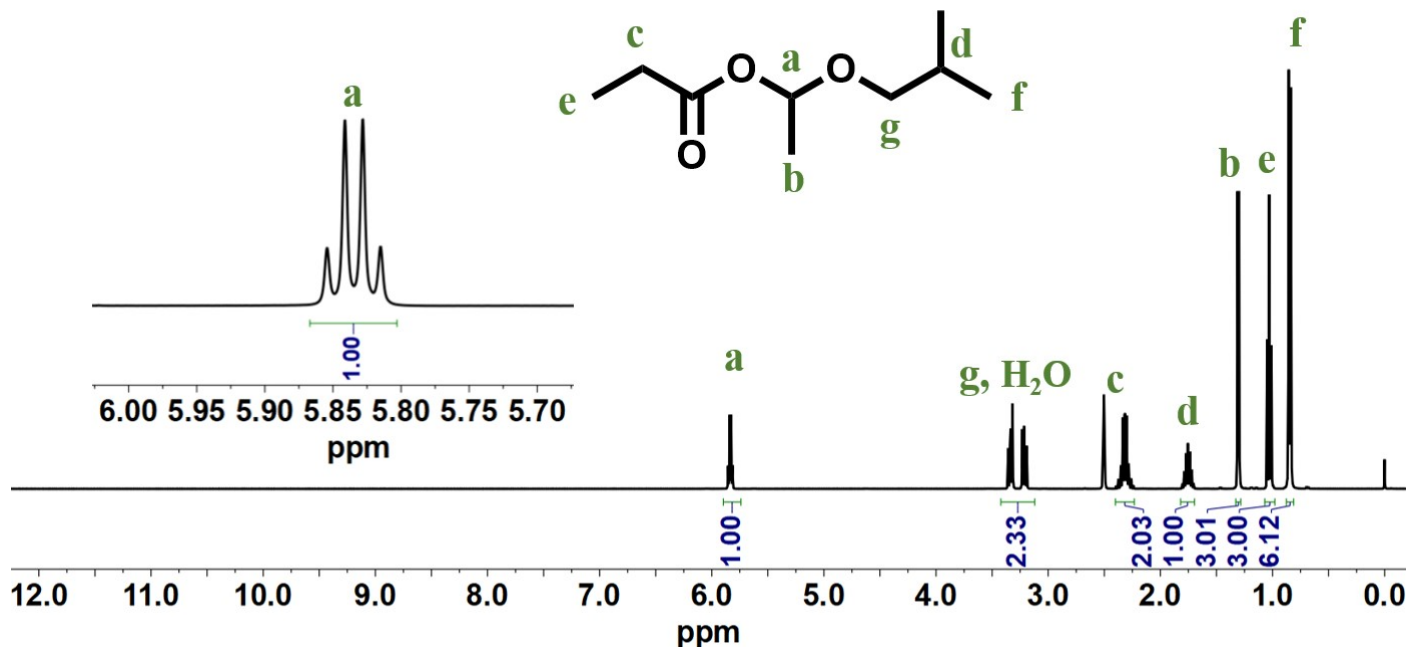


**Fig. S4**  $^1\text{H}$  NMR spectrum of PPA-IVE.

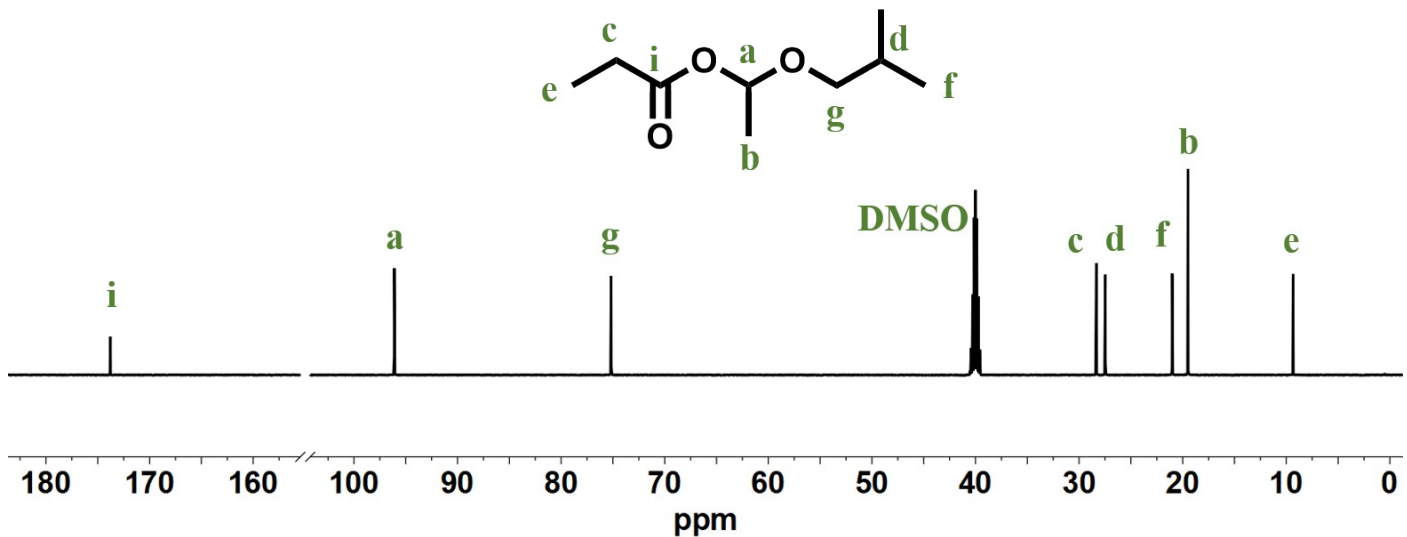


**Fig. S5**  $^{13}\text{C}$  NMR spectrum of PPA-IVE.

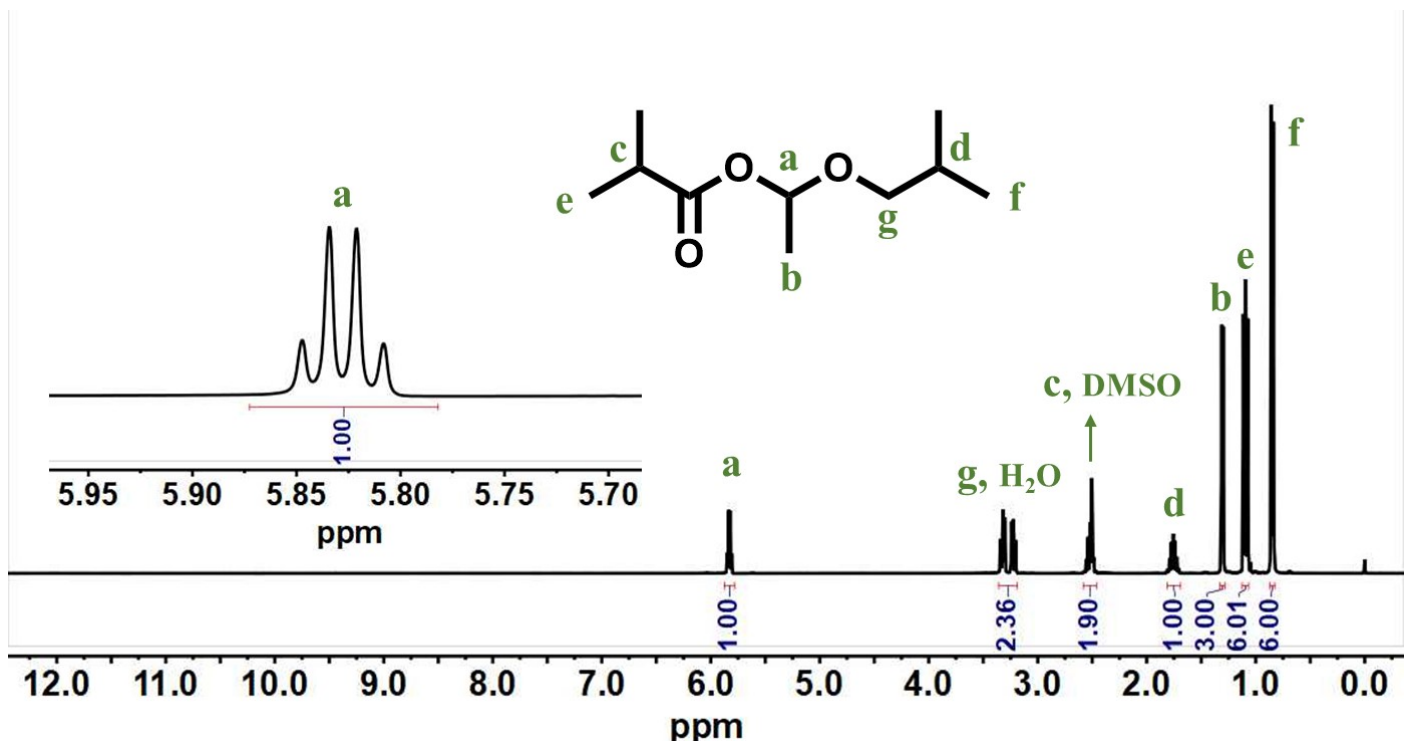


**Fig. S6**  $^1\text{H}$  NMR spectrum of IBA-IVE.

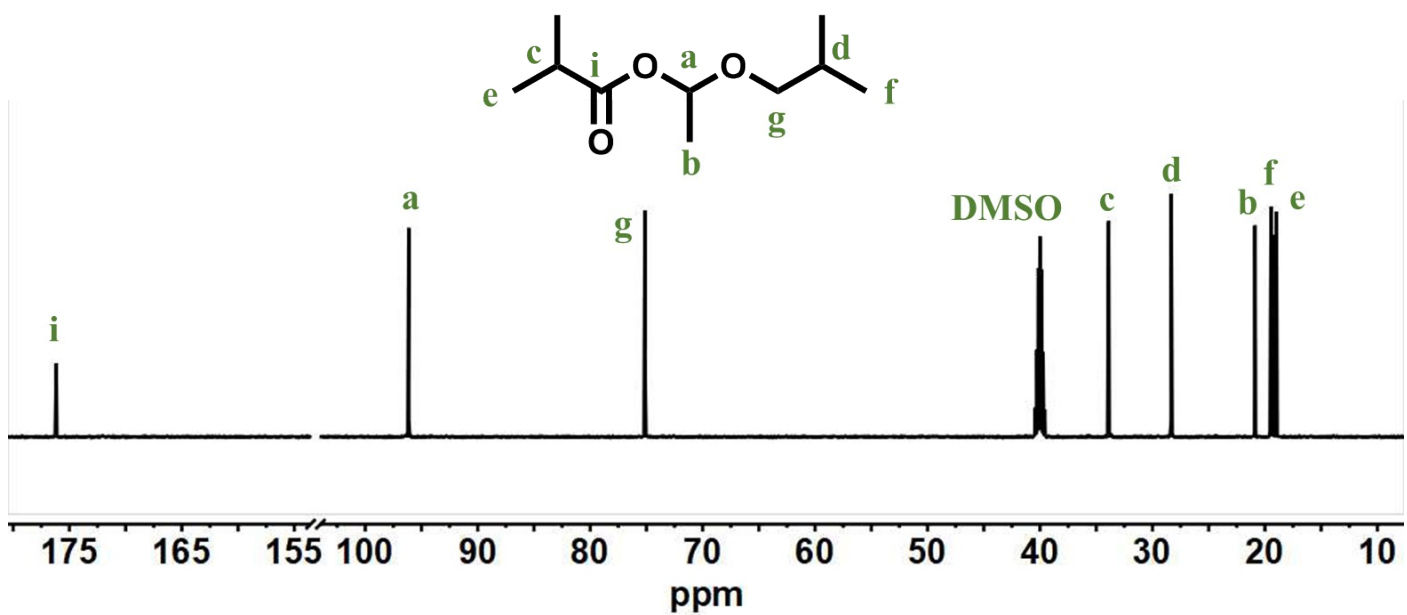


**Fig. S7**  $^{13}\text{C}$  NMR spectrum of IBA-IVE.

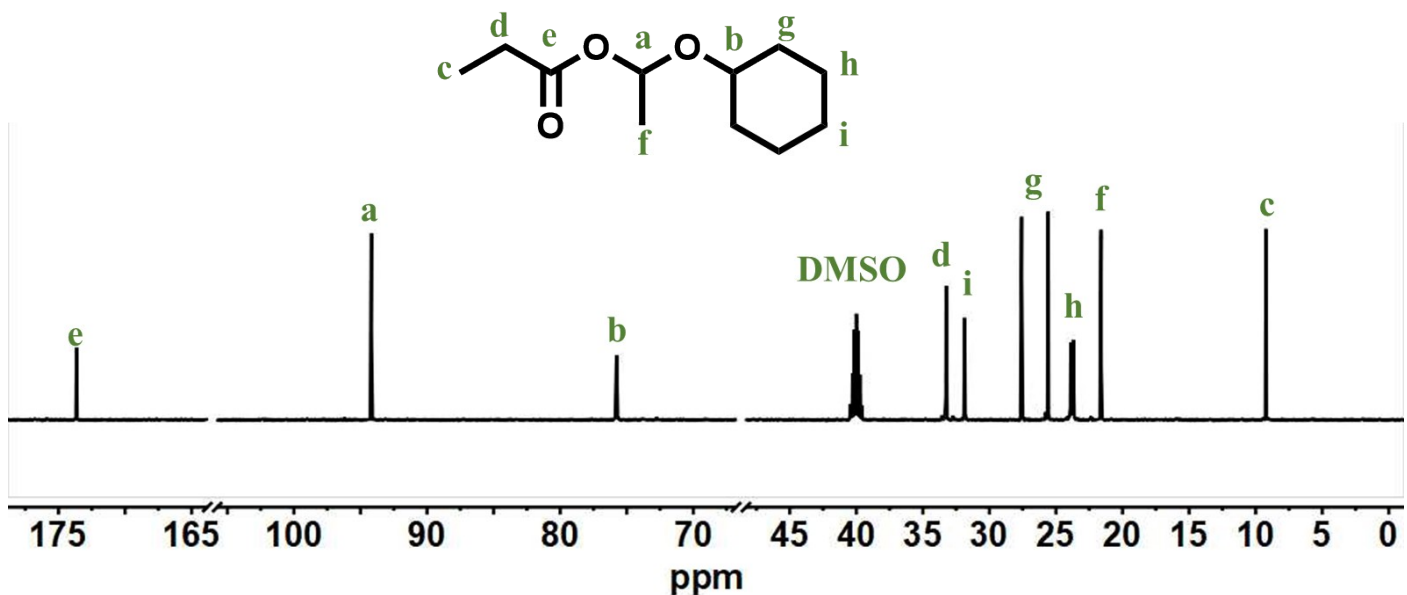


**Fig. S8**  $^1\text{H}$  NMR spectrum of PPA-CVE.

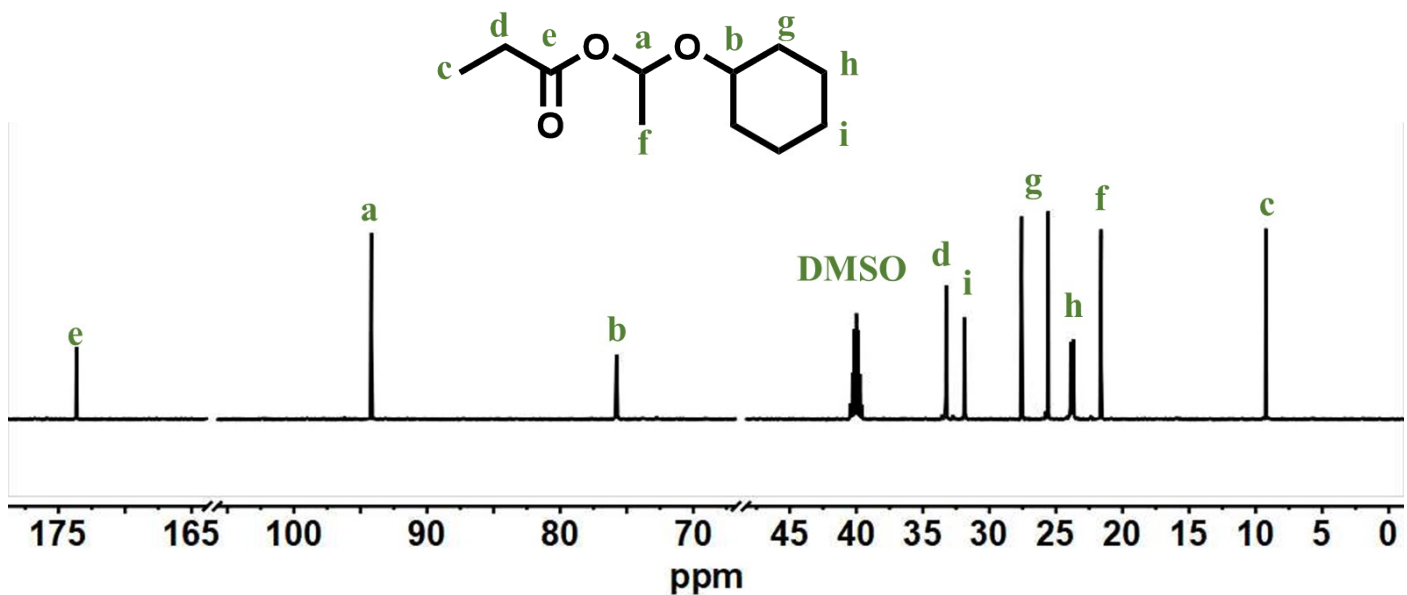


**Fig. S9**  $^{13}\text{C}$  NMR spectrum of PPA-CVE.

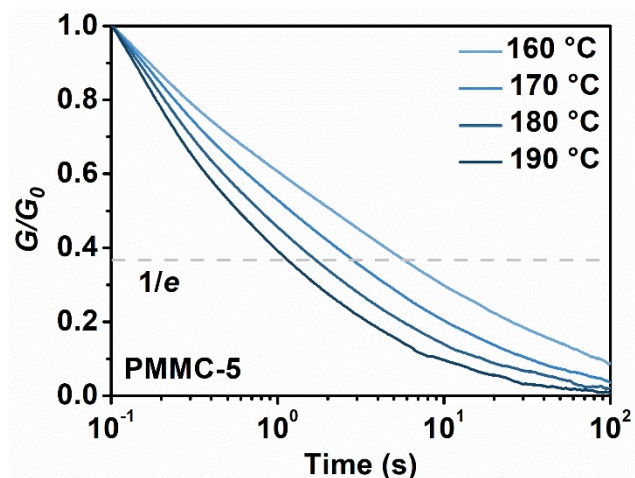


**Fig. S10** Stress relaxation curves of PMMC-5 at different temperatures.

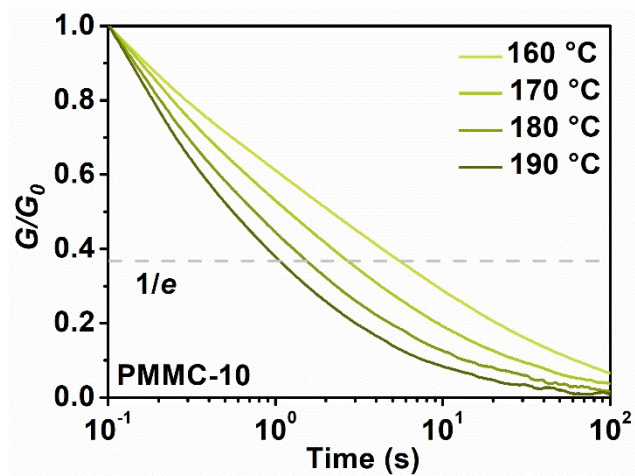


**Fig. S11** Stress relaxation curves of PMMC-10 at different temperatures.

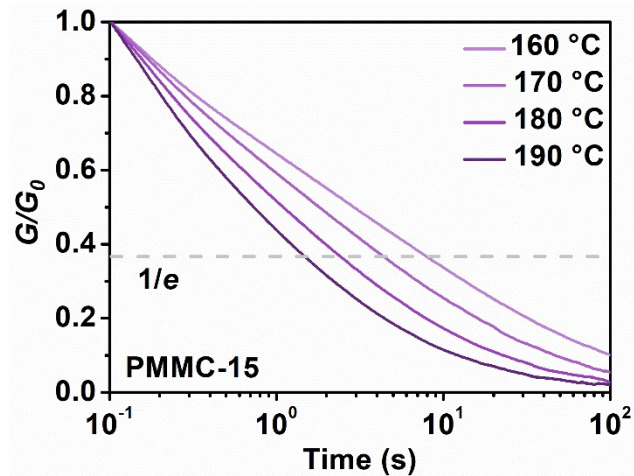


**Fig. S12** Stress relaxation curves of PMMC-15 at different temperatures.

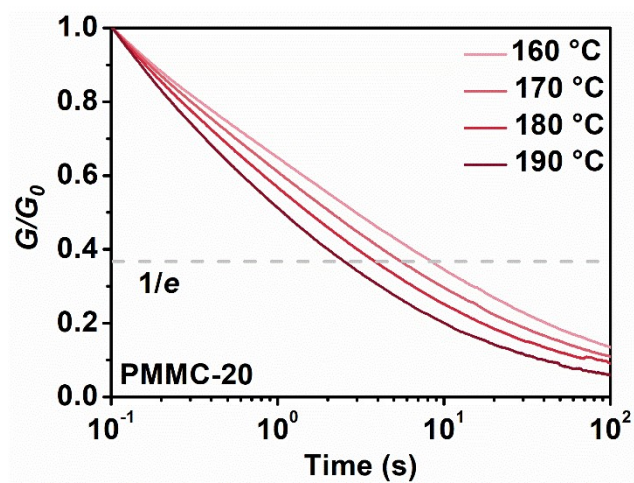


**Fig. S13** Stress relaxation curves of PMMC-20 at different temperatures.

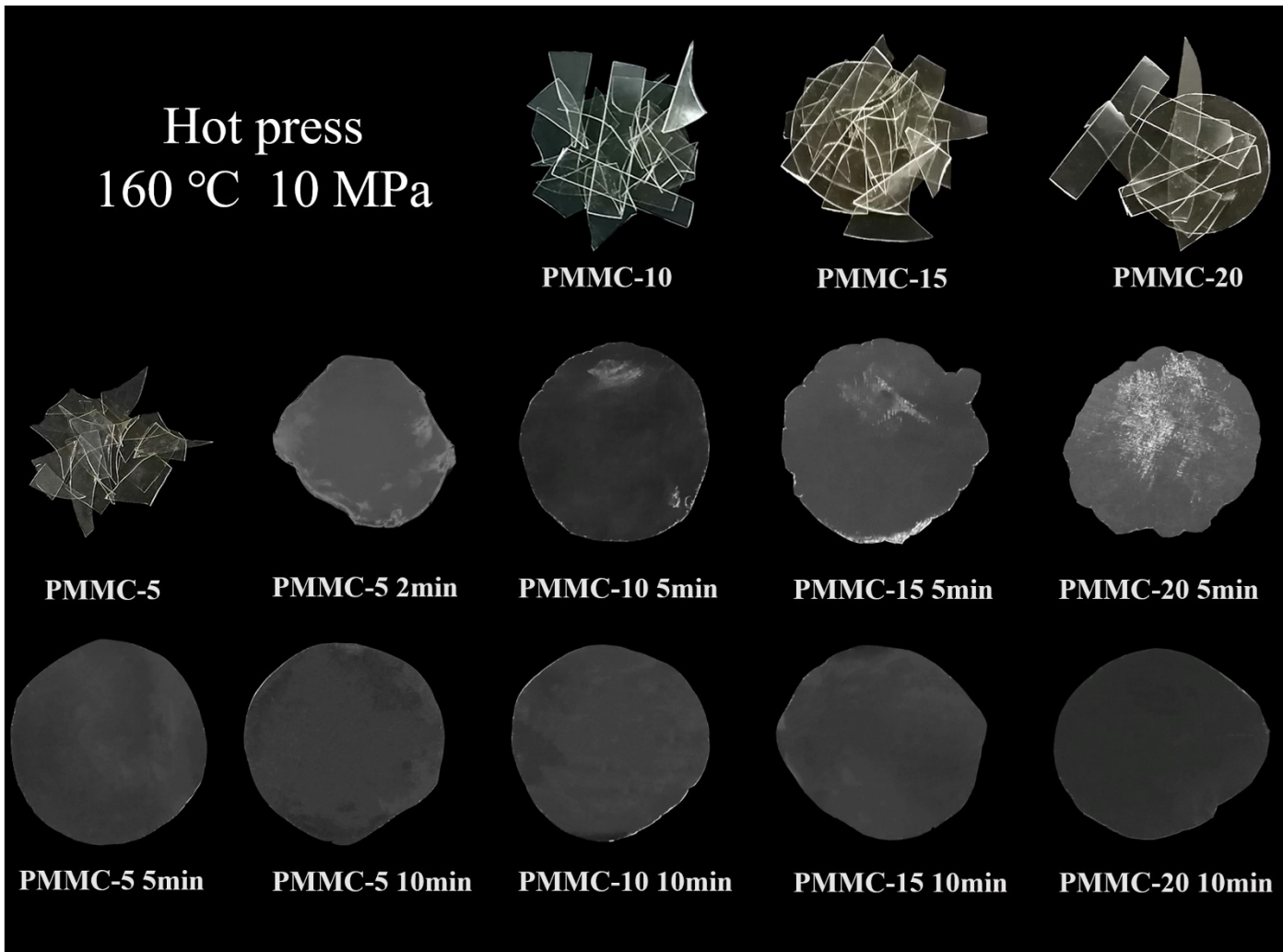


**Fig. S14** Reprocess recycling through hot press with different time.

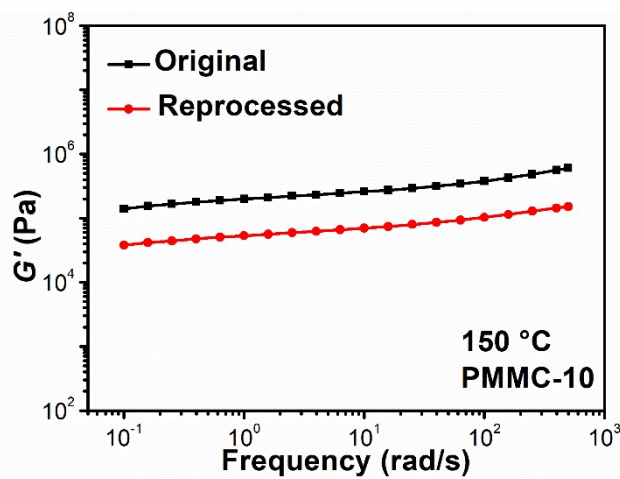


**Fig. S15** Frequency sweep measurements at 150 °C of the original and reprocessed (compression remolded) PMMC-10.

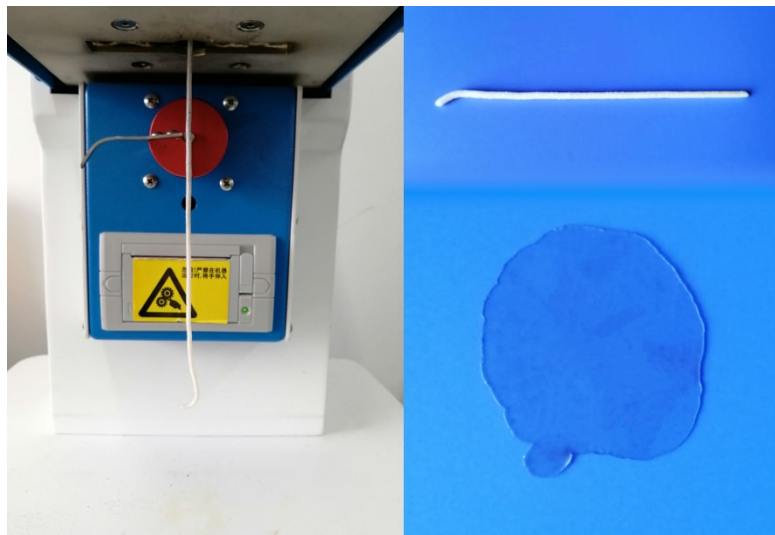


**Fig. S16** Reprocess recycling through extrusion plastometer and hot press at 160 °C for 10 min.

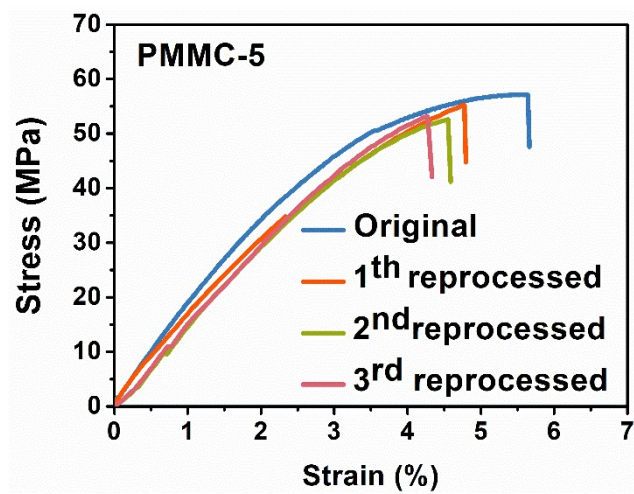


**Fig. S17** Representative tensile stress-strain curves of the original and reprocessed PMMC-5.

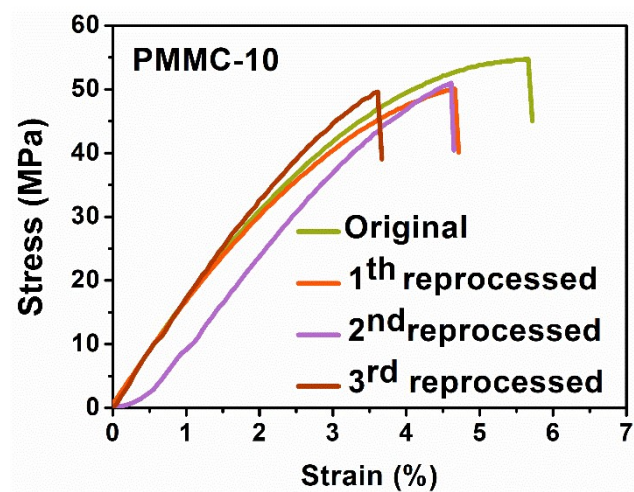


**Fig. S18** Representative tensile stress-strain curves of the original and reprocessed PMMC-10.

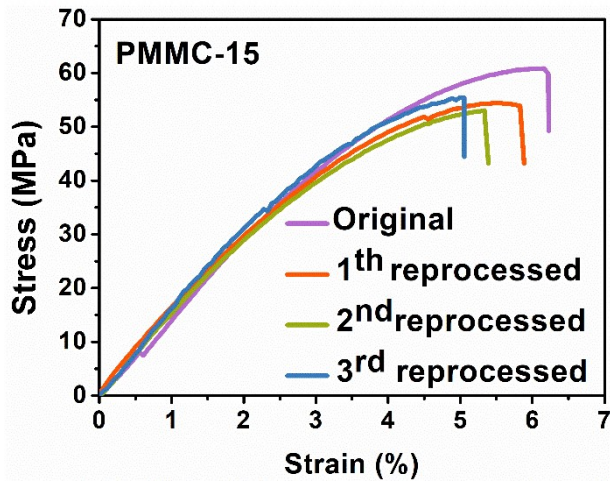


**Fig. S19** Representative tensile stress-strain curves of the original and reprocessed PMMC-15.

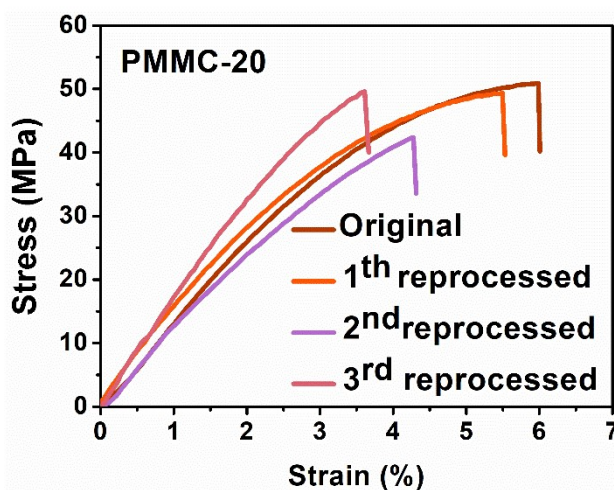


**Fig. S20** Representative tensile stress-strain curves of the original and reprocessed PMMC-20.

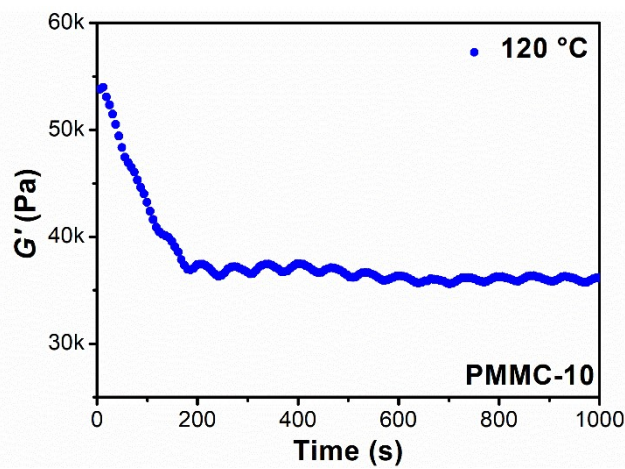


**Fig. S21** Time sweep measurement at 120 °C of the PMMC-10.

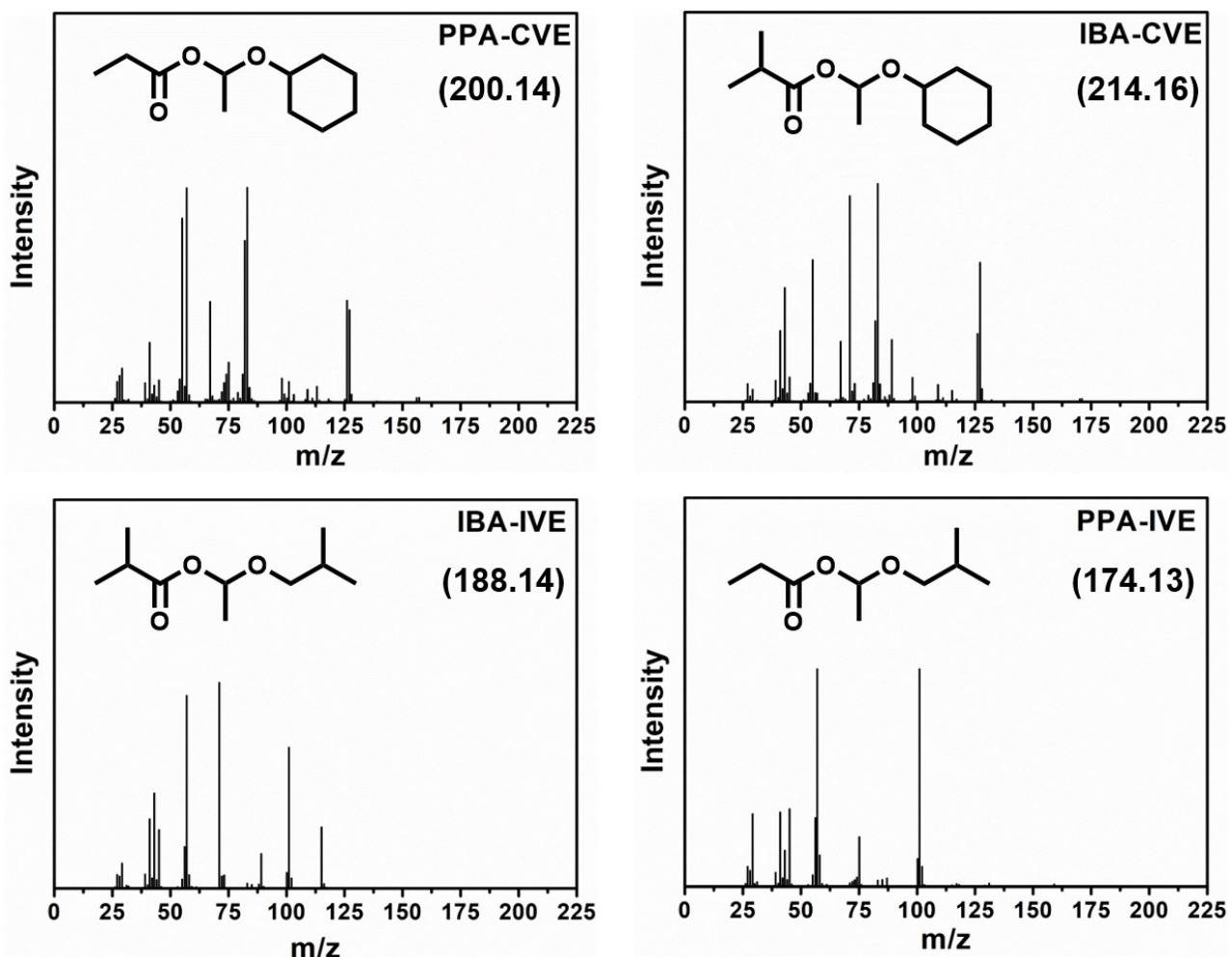


**Fig. S22** Mass spectra of PPA-IVE, IBA-CVE, IBA-IVE, PPA-CVE.

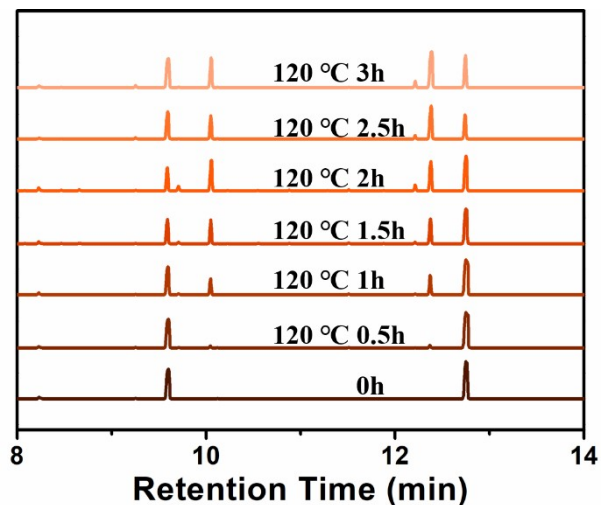


**Fig. S23** Gas chromatograms of metathesis without PPA at 120 °C for different time.

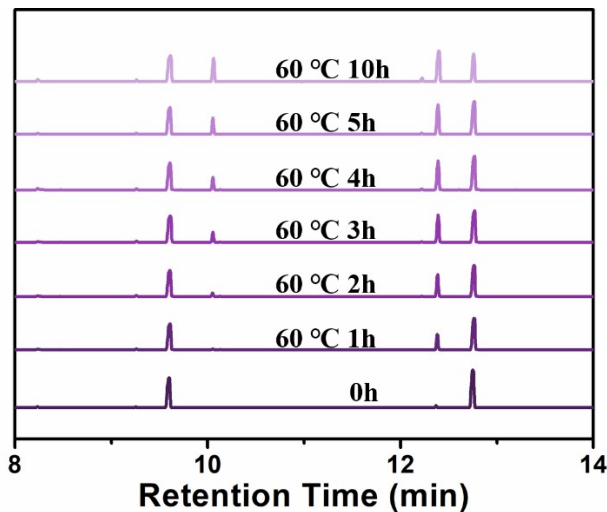


**Fig. S24** Gas chromatograms of metathesis with PPA at 60 °C for different time.

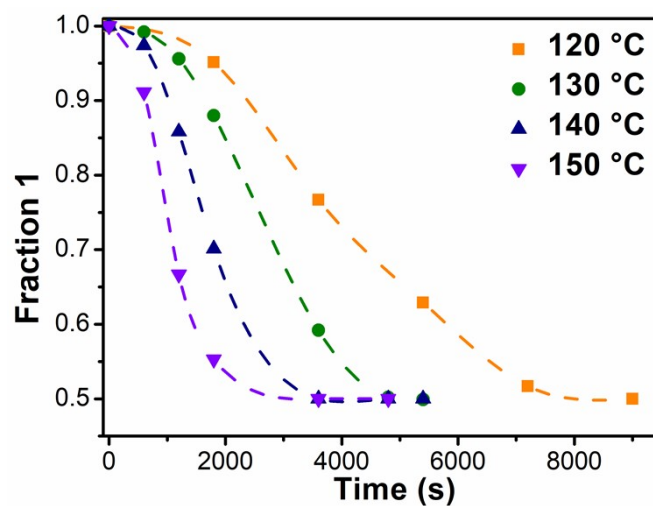


**Fig. S25** Fraction of 1 as a function of time during the exchange experiment at different temperatures.

As shown in the main text, this reaction can be described in terms of second-order kinetics (eq (1)). In addition, considering a vast excess of PPA-IVE, eq (1) can be transformed into eq (2). Small molecule IBA-CVE = **1**, PPA-IVE = **2**.

$$\frac{d[1]}{dt} = -k[1][2] \quad (1)$$

$$= -k_{exp}[1] \quad (2)$$

$k$ : rate constant,  $k_{exp}$ : experimental rate constant

If the initial concentration of **1** is described as  $[1]_0$ , eq (2) can be transformed to eq (3)<sup>1</sup>.

$$\ln\left(\frac{[1]}{[1]_0}\right) = -k_{exp} t \quad (3)$$

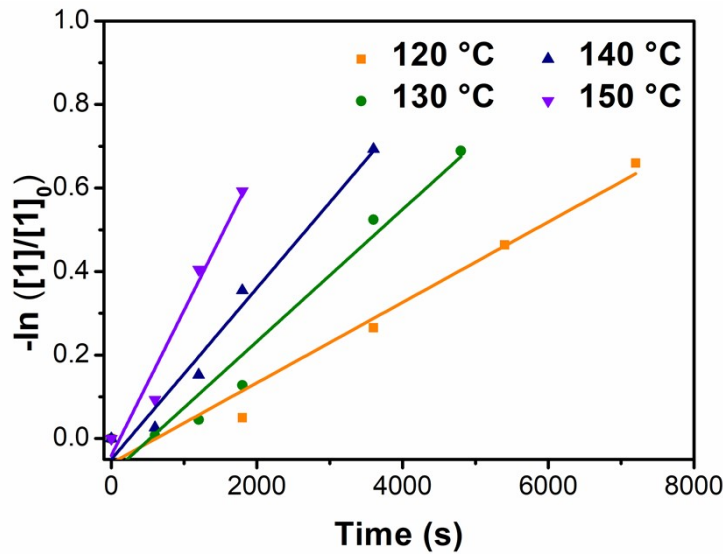


**Fig. S26** Plot of  $-\ln ([1]/[1]_0)$  versus  $t$  for the small molecule 1.  $k_{exp}$  at each temperature was determined by its slope value.

120 °C	$y = 0.0000962963x - 0.059$	$R^2 = 0.96$
130 °C	$y = 0.000158194x - 0.08401$	$R^2 = 0.95$
120 °C	$y = 0.000205213x - 0.05006$	$R^2 = 0.97$
120 °C	$y = 0.000348328x - 0.04085$	$R^2 = 0.95$

To calculate the activation energy for each reaction, the Arrhenius plots were made using  $k_{exp}$ .

$k = A \exp(-Ea/RT)$  ( $A$  : pre-exponential factor,  $Ea$  : activation energy,  $R$  : universal gas constant)  
 $R = 8.314 \text{ J K}^{-1} \text{ mol}^{-1}$  was used to calculate the activation energies from the slope values.

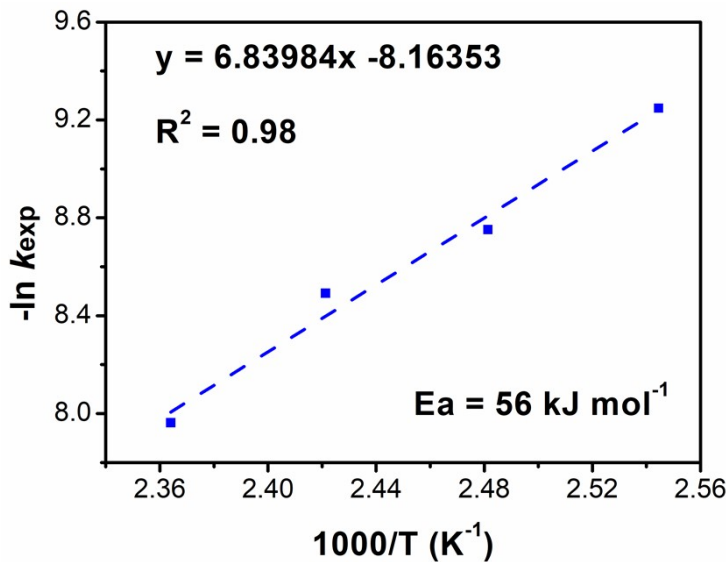


**Fig. S27** Arrhenius analysis of the rate constant  $k_{exp}$  versus  $T$  for 1 and 2 exchange.

**Table S1** Thermo-physical properties of different samples

Sample	$T_g$ (°C)	$v_e$ (mol cm <sup>-3</sup> )	$T_{d5\%}$ (°C)	$T_{d30\%}$ (°C)	$T_s$ (°C)
PMMC-5	126	154	238	379	158
PMMC-10	124	130	227	386	158
PMMC-15	117	114	217	388	157
PMMC-20	113	164	218	387	157

$$T_s = 0.49[T_{d5\%} + 0.6(T_{d30\%} - T_{d5\%})]$$

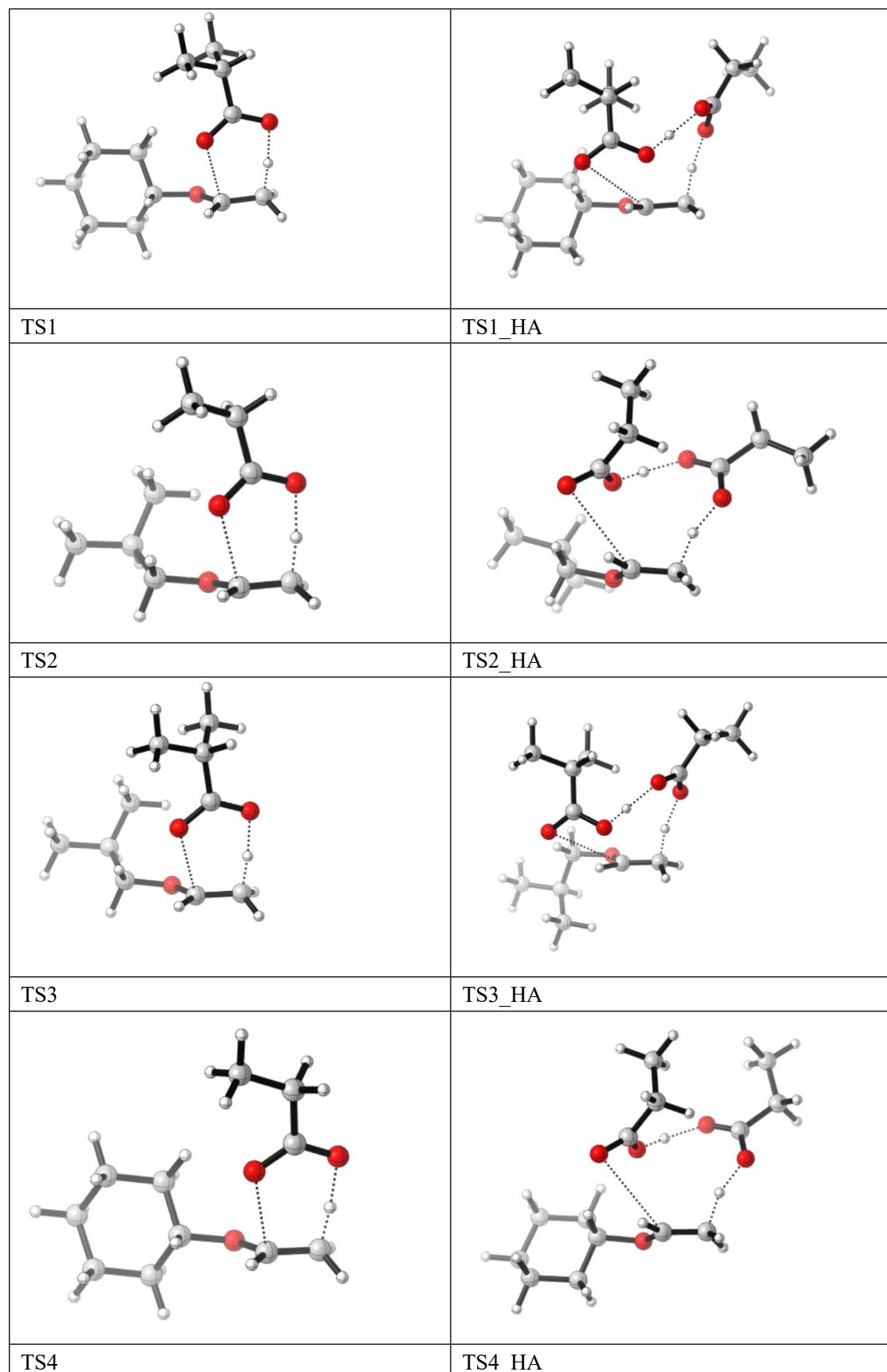
**Table S2** Mechanical properties of different samples

Sample	Young's modulus (MPa)	Tensile strength (MPa)	Elongation at break (%)
PMMC-5	1967±43	57±5	5.63±0.37
PMMC-10	1906±34	54±6	5.66±0.18
PMMC-15	1864±55	53±4	5.83±0.27
PMMC-20	1773±47	52±9	5.49±0.32

**Table S3** Mechanical properties of the original and reprocessed PMMC-5

Sample	Young's modulus (MPa)	Tensile strength (MPa)	Elongation at break (%)
Original	1967±43	57±5	5.43±0.32
Hot press	1827±60	55±8	4.79±0.45
Melt flow	1760±72	53±6	4.40±0.54
Extrude	1810±48	56±4	4.37±0.27

**Table S4** Transition state geometry



## References

- 1 Q. Li, S. Ma, P. Li, B. Wang, H. Feng, N. Lu, S. Wang, Y. Liu, X. Xu, J. Zhu, *Macromolecules*, 2021, **54**, 1742–1753.